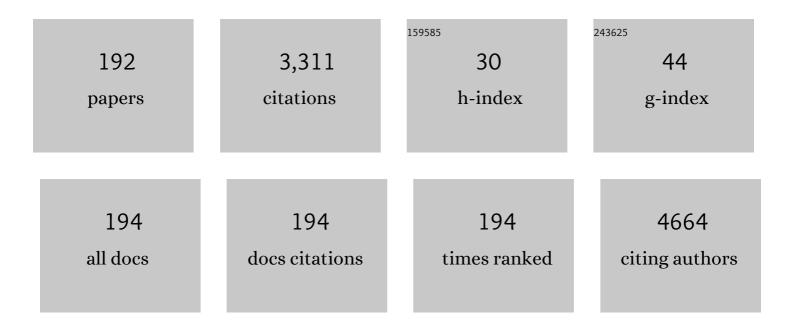
## Vladimir B Pavlovic

List of Publications by Year in descending order

Source: https://exaly.com/author-pdf/2939864/publications.pdf Version: 2024-02-01



#	Article	IF	CITATIONS
1	Properties of free-standing graphene oxide/silver nanowires films and effects of chemical reduction and gamma irradiation. Synthetic Metals, 2022, 283, 116980.	3.9	4
2	Photoactive graphene quantum dots/bacterial cellulose hydrogels: Structural, mechanical, and proâ€oxidant study. Journal of Applied Polymer Science, 2022, 139, 51996.	2.6	4
3	The Structuring of Sage (Salvia officinalis L.) Extract-Incorporating Edible Zein-Based Materials with Antioxidant and Antibacterial Functionality by Solvent Casting versus Electrospinning. Foods, 2022, 11, 390.	4.3	17
4	Removal of the As(V) and Sr(VI) from the water using magnetite/3D-printed wollastonite hybrid adsorbent. Science of Sintering, 2022, 54, 105-124.	1.4	3
5	Physico-chemical and mechanical properties of geopolymer/zircon composites. Science of Sintering, 2022, 54, 11-24.	1.4	1
6	Brushite-Metakaolin Composite Geopolymer Material as an Effective Adsorbent for Lead Removal from Aqueous Solutions. Sustainability, 2022, 14, 4003.	3.2	2
7	Structural Characterization of Nanocellulose/Fe3O4 Hybrid Nanomaterials. Polymers, 2022, 14, 1819.	4.5	7
8	Hydroxyapatite/TiO2 Nanomaterial with Defined Microstructural and Good Antimicrobial Properties. Antibiotics, 2022, 11, 592.	3.7	8
9	Hybrid amino-terminated lignin microspheres loaded with magnetite and manganese oxide nanoparticles: An effective hazardous oxyanions adsorbent. Journal of Environmental Chemical Engineering, 2022, 10, 108009.	6.7	6
10	Enzyme immobilization using two processing methods onto silica core-shell particles. Boletin De La Sociedad Espanola De Ceramica Y Vidrio, 2021, 60, 243-254.	1.9	8
11	Polymer-Ceramic Nanocomposites and Converging Technologies. , 2021, , 134-144.		3
12	Encapsulation of peach waste extract in Saccharomyces cerevisiae cells. Journal of the Serbian Chemical Society, 2021, 86, 367-380.	0.8	5
13	Design of halloysite modification for improvement of mechanical properties of the epoxy based nanocomposites. Polymer Composites, 2021, 42, 2180-2192.	4.6	15
14	Photoactive and antioxidant nanochitosan dots/biocellulose hydrogels for wound healing treatment. Materials Science and Engineering C, 2021, 122, 111925.	7.3	26
15	PVDF-HFP/NKBT composite dielectrics: Perovskite particles induce the appearance of an additional dielectric relaxation process in ferroelectric polymer matrix. Polymer Testing, 2021, 96, 107093.	4.8	15
16	High Heat Treatment of Goat Cheese Milk. The Effect on Sensory Profile, Consumer Acceptance and Microstructure of Cheese. Foods, 2021, 10, 1116.	4.3	4
17	Freeze vs. Spray Drying for Dry Wild Thyme (Thymus serpyllum L.) Extract Formulations: The Impact of Gelatin as a Coating Material. Molecules, 2021, 26, 3933.	3.8	21
18	Optimization of the synthesis parameters of nanocomposites based on bacterial nanocellulose/Fe3O4. Tehnika, 2021, 76, 273-278.	0.2	0

#	Article	IF	CITATIONS
19	High-performance laminate material based on polyurethane and epoxide reinforced by silica particles from rice husk used for intelligent pedestrian crossings. Iranian Polymer Journal (English Edition), 2021, 30, 319-330.	2.4	9
20	SINTEZA I STRUKTURA BAKTERIJSKE CELULOZE PRIMENOM BAKTERIJA SIRĆETNOG VRENJA. , 2021, , .		1
21	Evaluation of adsorption performance and quantum chemical modeling of pesticides removal using Cell-MG hybrid adsorbent. Science of Sintering, 2021, 53, 355-378.	1.4	4
22	Novel magnetic polymer/bentonite composite: Characterization and application for Re(VII) and W(VI) adsorption. Science of Sintering, 2021, 53, 419-428.	1.4	2
23	Potential Usage of Hybrid Polymers Binders Based on Fly Ash with the Addition of PVA with Satisfying Mechanical and Radiological Properties. Gels, 2021, 7, 270.	4.5	3
24	Enhanced accessibility of active sites in hierarchical ZSM-5 zeolite for removal of pharmaceutically active substances: Adsorption and microcalorimetric study. Arabian Journal of Chemistry, 2020, 13, 1945-1954.	4.9	16
25	Formation kinetics and cation inversion in mechanically activated MgAl2O4 spinel ceramics. Journal of Thermal Analysis and Calorimetry, 2020, 140, 95-107.	3.6	7
26	Graphene quantum dots as singlet oxygen producer or radical quencher - The matter of functionalization with urea/thiourea. Materials Science and Engineering C, 2020, 109, 110539.	7.3	42
27	Highly Efficient Antioxidant F- and Cl-Doped Carbon Quantum Dots for Bioimaging. ACS Sustainable Chemistry and Engineering, 2020, 8, 16327-16338.	6.7	71
28	Rheology and Microstructures of Rennet Gels from Differently Heated Goat Milk. Foods, 2020, 9, 283.	4.3	13
29	Altered organization of collagen fibers in the uninvolved human colon mucosa 10 cm and 20 cm away from the malignant tumor. Scientific Reports, 2020, 10, 6359.	3.3	24
30	Study of nanosized hydroxyapatite material annealing at different retention times. Science of Sintering, 2020, 52, 405-413.	1.4	3
31	One-pot combustion synthesis of nickel oxide and hematite: From simple coordination compounds to high purity metal oxide nanoparticles. Science of Sintering, 2020, 52, 481-490.	1.4	8
32	TiO2 based nanomaterials and nanostructures for green convergent technologies and environmental protection. Materials Protection, 2020, 61, 346-355.	0.9	0
33	Nanocrystalline Zn2SnO4/SnO2: Crystal structure and humidity influence on complex impedance. Journal of Electroceramics, 2020, 45, 135-147.	2.0	3
34	Effects of mechanical activation on the formation and sintering kinetics of barium strontium titanate ceramics. Science of Sintering, 2020, 52, 371-385.	1.4	6
35	Structure and enhanced antimicrobial activity of mechanically activated nano TiO <sub>2</sub> . Journal of the American Ceramic Society, 2019, 102, 7735-7745.	3.8	10
36	Graphene oxide size and structure pro-oxidant and antioxidant activity and photoinduced cytotoxicity relation on three cancer cell lines. Journal of Photochemistry and Photobiology B: Biology, 2019, 200, 111647.	3.8	39

#	Article	IF	CITATIONS
37	Influence of different concentrations of Zn-carbonate phase on physical-chemical properties of antimicrobial agar composite films. Materials Letters, 2019, 255, 126572.	2.6	4
38	Tailoring the physico-chemical and antimicrobial properties of agar-based films by in situ formation of Cu-mineral phase. European Polymer Journal, 2019, 119, 352-358.	5.4	7
39	Production of bacterial nanocellulose (BNC) and its application as a solid support in transition metal catalysed cross-coupling reactions. International Journal of Biological Macromolecules, 2019, 129, 351-360.	7.5	33
40	Characterisation of peppermint ( <i>Mentha piperita</i> L.) essential oil encapsulates. Journal of Microencapsulation, 2019, 36, 109-119.	2.8	41
41	Controllable synthesis of Fe3O4-wollastonite adsorbents for efficient heavy metal ions/oxyanions removal. Environmental Science and Pollution Research, 2019, 26, 12379-12398.	5.3	10
42	Polyamidoamine as a clay modifier and curing agent in preparation of epoxy nanocomposites. Progress in Organic Coatings, 2019, 131, 311-321.	3.9	16
43	Synthesis and characterization of BaTiO3/α-Fe2O3 core/shell structure. Journal of Advanced Ceramics, 2019, 8, 133-147.	17.4	10
44	Effects of mechanical-activation and TiO2 addition on the behavior of two-step sintered steatite ceramics. Ceramics International, 2019, 45, 3013-3022.	4.8	1
45	Processing and properties of dense cordierite ceramics obtained through solid-state reaction and pressure-less sintering. Advances in Applied Ceramics, 2019, 118, 241-248.	1.1	10
46	Kinetics of thermally activated processes in cordierite-based ceramics. Journal of Thermal Analysis and Calorimetry, 2019, 138, 2989-2998.	3.6	7
47	Arsenic removal by magnetite-loaded amino modified nano/microcellulose adsorbents: Effect of functionalization and media size. Arabian Journal of Chemistry, 2019, 12, 4675-4693.	4.9	64
48	Modification of graphene oxide surfaces with 12-molybdophosphoric acid: Structural and antibacterial study. Materials Chemistry and Physics, 2018, 213, 157-167.	4.0	14
49	Enhancement of nano titanium dioxide coatings by fullerene and polyhydroxy fullerene in the photocatalytic degradation of the herbicide mesotrione. Chemosphere, 2018, 196, 145-152.	8.2	23
50	Influence of mechanical activation on functional properties of barium hexaferrite ceramics. Ceramics International, 2018, 44, 6666-6672.	4.8	9
51	Dispersion efficiency of montmorillonites in epoxy nanocomposites using solution intercalation and direct mixing methods. Applied Clay Science, 2018, 154, 52-63.	5.2	17
52	Hepatoprotective effect of fullerenol/doxorubicin nanocomposite in acute treatment of healthy rats. Experimental and Molecular Pathology, 2018, 104, 199-211.	2.1	15
53	A high-sensitive current-mode pressure/force detector based on piezoelectric polymer PVDF. Sensors and Actuators A: Physical, 2018, 276, 165-175.	4.1	22
54	Bimetallic alginate nanocomposites: New antimicrobial biomaterials for biomedical application. Materials Letters, 2018, 212, 32-36.	2.6	17

#	Article	IF	CITATIONS
55	Customizing the spent coffee for Trichoderma reesei cellulase immobilization by modification with activating agents. International Journal of Biological Macromolecules, 2018, 107, 1856-1863.	7.5	8
56	Humidity sensing properties of nanocrystalline pseudobrookite (Fe2TiO5) based thick films. Sensors and Actuators B: Chemical, 2018, 277, 654-664.	7.8	39
57	Photo-induced antibacterial activity of four graphene based nanomaterials on a wide range of bacteria. RSC Advances, 2018, 8, 31337-31347.	3.6	69
58	Crossâ€Linkable Modified Nanocellulose/Polyester Resinâ€Based Composites: Effect of Unsaturated Fatty Acid Nanocellulose Modification on Material Performances. Macromolecular Materials and Engineering, 2018, 303, 1700648.	3.6	15
59	DUV fluorescence bioimaging study of the interaction of partially reduced graphene oxide and liver cancer cells. 2D Materials, 2018, 5, 045019.	4.4	3
60	Structural and electrical properties of ferroelectric poly(vinylidene fluoride) and mechanically activated ZnO nanoparticle composite films. Physica Scripta, 2018, 93, 105801.	2.5	25
61	Simple route for the preparation of graphene/poly(styreneâ€∢i>bâ€butadieneâ€∢i>bâ€styrene) nanocomposite films with enhanced electrical conductivity and hydrophobicity. Polymer International, 2018, 67, 1118-1127.	3.1	4
62	Effect of chemical composition on microstructural properties and sintering kinetics of (Ba,Sr)TiO3 powders. Science of Sintering, 2018, 50, 29-38.	1.4	2
63	Structure and photocatalytic properties of sintered TiO2 nanotube arrays. Science of Sintering, 2018, 50, 39-50.	1.4	8
64	Microstructure and phase composition of steatite ceramics sintered by traditional and spark plasma sintering. Science of Sintering, 2018, 50, 299-312.	1.4	5
65	Physical properties of sintered alumina doped with different oxides. Science of Sintering, 2018, 50, 409-419.	1.4	10
66	Effect of the vinyl modification of multi-walled carbon nanotubes on the performances of waste poly(ethylene terephthalate)-based nanocomposites. Journal of Composite Materials, 2017, 51, 491-505.	2.4	12
67	Structural properties of the multiwall carbon nanotubes/poly(methyl methacrylate) nanocomposites: Effect of the multiwall carbon nanotubes covalent functionalization. Polymer Composites, 2017, 38, E472.	4.6	10
68	Structure analysis of geopolymers synthesized from clay originated from Serbia. Environmental Earth Sciences, 2017, 76, 1.	2.7	19
69	The impedance analysis of sintered MgTiO3 ceramics. Journal of Alloys and Compounds, 2017, 701, 107-115.	5.5	9
70	Novel modified nanocellulose applicable as reinforcement in high-performance nanocomposites. Carbohydrate Polymers, 2017, 164, 64-74.	10.2	32
71	Synthesis and antimicrobial properties of Zn-mineralized alginate nanocomposites. Carbohydrate Polymers, 2017, 165, 313-321.	10.2	41
72	Selective Al-Ti reactivity in laser-processed Al/Ti multilayers. Materials and Manufacturing Processes, 2017, 32, 1622-1627.	4.7	2

#	Article	IF	CITATIONS
73	Structural and chemical properties of thermally treated geopolymer samples. Ceramics International, 2017, 43, 6700-6708.	4.8	109
74	Selective magnetic GMA based potential sorbents for molybdenum and rhenium sorption. Journal of Alloys and Compounds, 2017, 705, 38-50.	5.5	28
75	Antibacterial potential of electrochemically exfoliated graphene sheets. Journal of Colloid and Interface Science, 2017, 500, 30-43.	9.4	31
76	Influence of different pore-forming agents on wollastonite microstructures and adsorption capacities. Ceramics International, 2017, 43, 7461-7468.	4.8	21
77	Improvement of mechanical properties and antibacterial activity of crosslinked electrospun chitosan/poly (ethylene oxide) nanofibers. Composites Part B: Engineering, 2017, 121, 58-67.	12.0	49
78	Montmorillonite/poly(urethane-siloxane) nanocomposites: Morphological, thermal, mechanical and surface properties. Applied Clay Science, 2017, 149, 136-146.	5.2	34
79	Effects of different carrier materials on physicochemical properties of microencapsulated grape skin extract. Journal of Food Science and Technology, 2017, 54, 3411-3420.	2.8	43
80	Microencapsulation of anthocyanin-rich black soybean coat extract by spray drying using maltodextrin, gum Arabic and skimmed milk powder. Journal of Microencapsulation, 2017, 34, 475-487.	2.8	36
81	Ambient light induced antibacterial action of curcumin/graphene nanomesh hybrids. RSC Advances, 2017, 7, 36081-36092.	3.6	31
82	Influence of different bonding and fluxing agents on the sintering behavior and dielectric properties of steatite ceramic materials. Ceramics International, 2017, 43, 13264-13275.	4.8	10
83	Mineralized agar-based nanocomposite films: Potential food packaging materials with antimicrobial properties. Carbohydrate Polymers, 2017, 175, 55-62.	10.2	59
84	Fatty acids of maize pollen – Quantification, nutritional and morphological evaluation. Journal of Cereal Science, 2017, 77, 180-185.	3.7	25
85	Optimization of bentonite clay mechano-chemical activation using artificial neural network modeling. Ceramics International, 2017, 43, 2549-2562.	4.8	14
86	The influence of mechanical activation on structural evolution of nanocrystalline SrTiO3 powders. Journal of Alloys and Compounds, 2017, 695, 863-870.	5.5	24
87	Dielectric properties, complex impedance and electrical conductivity of Fe2TiO5 nanopowder compacts and bulk samples at elevated temperatures. Journal of Materials Science: Materials in Electronics, 2017, 28, 4796-4806.	2.2	19
88	Sintering of fly ash based composites with zeolite and bentonite addition for application in construction materials. Science of Sintering, 2017, 49, 23-37.	1.4	5
89	Formation of porous wollastonite-based ceramics after sintering with yeast as the pore-forming agent. Science of Sintering, 2017, 49, 235-246.	1.4	4
90	Characterisation of Mn0.63Zn0.37Fe2O4 powders after intensive milling and subsequent thermal treatment. Science of Sintering, 2017, 49, 455-467.	1.4	2

#	Article	IF	CITATIONS
91	Electrical properties of magnesium titanate ceramics post-sintered by hot isostatic pressing. Science of Sintering, 2017, 49, 373-380.	1.4	0
92	Characterization of FeCoV alloy processed by PIM/MIM route. Science of Sintering, 2017, 49, 299-309.	1.4	0
93	Gelatin as a carrier system for delivery of polyphenols compounds. Tehnika, 2017, 72, 633-639.	0.2	0
94	Adsorption of Organophosphate Pesticide Dimethoate on Gold Nanospheres and Nanorods. Journal of Nanomaterials, 2016, 2016, 1-11.	2.7	43
95	The Antibacterial Activity of Coriolus versicolor Methanol Extract and Its Effect on Ultrastructural Changes of Staphylococcus aureus and Salmonella Enteritidis. Frontiers in Microbiology, 2016, 7, 1226.	3.5	66
96	Zirconium dioxide nanopowders with incorporated Si4+ ions as efficient photocatalyst for degradation of trichlorophenol using simulated solar light. Applied Catalysis B: Environmental, 2016, 195, 112-120.	20.2	43
97	Optical properties of spherical quantum dot with on-center hydrogen impurity in magnetic field. Optical and Quantum Electronics, 2016, 48, 1.	3.3	9
98	The influence of mechanical activation on the morphological changes of Fe/BaTiO3 powder. Materials Science and Engineering B: Solid-State Materials for Advanced Technology, 2016, 212, 89-95.	3.5	3
99	Synthesis and characterization of a new type of levan-graft-polystyrene copolymer. Carbohydrate Polymers, 2016, 154, 20-29.	10.2	19
100	SYNTHESIS AND CHARACTERIZATION OF ELECTROCHEMICALLY EXFOLIATED GRAPHENE-MOLYBDOPHOSPHATE HYBRID MATERIALS FOR CHARGE STORAGE DEVICES. Electrochimica Acta, 2016, 217, 34-46.	5.2	4
101	Effects of mechanical activation and two-step sintering on the structure and electrical properties of cordierite-based ceramics. Ceramics International, 2016, 42, 13909-13918.	4.8	30
102	Effect of consolidation parameters on structural, microstructural and electrical properties of magnesium titanate ceramics. Ceramics International, 2016, 42, 9887-9898.	4.8	16
103	Reaction kinetics of mechanically activated cordierite-based ceramics studied via DTA. Journal of Thermal Analysis and Calorimetry, 2016, 124, 667-673.	3.6	7
104	Raman spectroscopy study of graphene thin films synthesized from solid precursor. Optical and Quantum Electronics, 2016, 48, 1.	3.3	6
105	Advances in batch culture fermented Coriolus versicolor medicinal mushroom for the production of antibacterial compounds. Innovative Food Science and Emerging Technologies, 2016, 34, 1-8.	5.6	27
106	CdS quantum dots sensitized TiO2 nanotubes by matrix assisted pulsed laser evaporation method. Ceramics International, 2016, 42, 9011-9017.	4.8	9
107	Functionalization of zinc ferrite nanoparticles: Influence of modification procedure on colloidal stability. Processing and Application of Ceramics, 2016, 10, 287-293.	0.8	20
108	Microstructural and electrical properties of cordierite-based ceramics obtained after two-step sintering technique. Science of Sintering, 2016, 48, 157-165.	1.4	9

#	Article	IF	CITATIONS
109	High performances unsaturated polyester based nanocomposites: Effect of vinyl modified nanosilica on mechanical properties. EXPRESS Polymer Letters, 2016, 10, 139-159.	2.1	49
110	Influence of mechanical activation on MgO-Al2O3-SiO2 system in the presence of TeO2 additive. Tehnika, 2016, 71, 797-802.	0.2	1
111	Novel Utilization of Fly Ash for Highâ€Temperature Mortars: Phase Composition, Microstructure and Performances Correlation. International Journal of Applied Ceramic Technology, 2015, 12, 133-146.	2.1	17
112	Thermally induced crystallization of amorphous Fe40Ni40P14B6 alloy. Thermochimica Acta, 2015, 614, 129-136.	2.7	12
113	Structural investigation of mechanically activated ZnO powder. Journal of Alloys and Compounds, 2015, 648, 971-979.	5.5	11
114	Protein-reinforced and chitosan-pectin coated alginate microparticles for delivery of flavan-3-ol antioxidants and caffeine from green tea extract. Food Hydrocolloids, 2015, 51, 361-374.	10.7	68
115	Investigation of thermally induced processes in corundum refractory concretes with addition of fly ash. Journal of Thermal Analysis and Calorimetry, 2015, 119, 1339-1352.	3.6	7
116	The effect of annealing temperature and time on synthesis of graphene thin films by rapid thermal annealing. Synthetic Metals, 2015, 209, 461-467.	3.9	21
117	Modification of Structural and Luminescence Properties of Graphene Quantum Dots by Gamma Irradiation and Their Application in a Photodynamic Therapy. ACS Applied Materials & Interfaces, 2015, 7, 25865-25874.	8.0	94
118	Biological potential of extracts of the wild edible Basidiomycete mushroom Grifola frondosa. Food Research International, 2015, 67, 272-283.	6.2	68
119	Characterization of sodium alginate/d-limonene emulsions and respective calcium alginate/d-limonene beads produced by electrostatic extrusion. Food Hydrocolloids, 2015, 45, 111-123.	10.7	59
120	Depth distribution of available micronutrients in cultivated soil. Journal of Agricultural Sciences (Belgrade), 2015, 60, 177-187.	0.3	5
121	The influence of compaction pressure on the density and electrical properties of cordierite-based ceramics. Science of Sintering, 2015, 47, 15-22.	1.4	5
122	Monolayer graphene films through nickel catalyzed transformation of fullerol and graphene quantum dots: a Raman spectroscopy study. Physica Scripta, 2014, T162, 014030.	2.5	8
123	Tuning the acidity of niobia: Characterization and catalytic activity of Nb2O5–MeO2 (MeÂ=ÂTi, Zr, Ce) mesoporous mixed oxides. Materials Chemistry and Physics, 2014, 146, 337-345.	4.0	37
124	Raman Responses in Mechanically Activated <scp><scp>BaTiO</scp></scp> <sub>3</sub> . Journal of the American Ceramic Society, 2014, 97, 601-608.	3.8	19
125	Thermal, morphological, and mechanical properties of ethyl vanillin immobilized in polyvinyl alcohol by electrospinning process. Journal of Thermal Analysis and Calorimetry, 2014, 118, 661-668.	3.6	23
126	Ferroelectric nanocomposites of polyvinylidene fluoride/polymethyl methacrylate blend and BaTiO3 particles: Fabrication of β-crystal polymorph rich matrix through mechanical activation of the filler. Journal of Applied Physics, 2014, 115, .	2.5	48

#	Article	IF	CITATIONS
127	Microstructure and Dielectric Properties of Rare-Earth Doped BaTiO <sub>3</sub> Ceramics. Ferroelectrics, 2014, 470, 159-167.	0.6	8
128	Preparation of PEDOT:PSS thin films doped with graphene and graphene quantum dots. Synthetic Metals, 2014, 198, 150-154.	3.9	27
129	The influence of mechanical activation on the electrical properties of Ba0.77Sr0.23TiO3 ceramics. Ceramics International, 2014, 40, 11883-11888.	4.8	5
130	Fractal corrections of BaTiO3-ceramic sintering parameters. Science of Sintering, 2014, 46, 149-156.	1.4	7
131	Advantages of combined sintering compared to conventional sintering of mechanically activated magnesium titanate. Science of Sintering, 2014, 46, 283-290.	1.4	5
132	Synthesis of magnesium titanates by mechanochemical method. Tehnika, 2014, 69, 727-731.	0.2	0
133	Cesium removal from aqueous solution by natural mineral clinoptilolite. Nuclear Technology and Radiation Protection, 2014, 29, 135-141.	0.8	0
134	Butterfly scales as bionic templates for complex ordered nanophotonic materials: A pathway to biomimetic plasmonics. Optical Materials, 2013, 35, 1869-1875.	3.6	6
135	Structural characterization and electrical properties of sintered magnesium–titanate ceramics. Journal of Alloys and Compounds, 2013, 555, 39-44.	5.5	9
136	Facile synthesis of poly(ε-caprolactone) micro and nanospheres using different types of polyelectrolytes as stabilizers under ambient and elevated temperature. Composites Part B: Engineering, 2013, 45, 1471-1479.	12.0	15
137	Depth Distribution of 137Cs in Anthrosol from the Experimental Field "Radmilovac―Near Belgrade, Serbia. Arhiv Za Higijenu Rada I Toksikologiju, 2013, 64, 425-430.	0.7	7
138	Structural properties of composites of polyvinylidene fluoride and mechanically activated BaTiO <sub>3</sub> particles. Physica Scripta, 2013, T157, 014006.	2.5	31
139	Electronic ceramic structure within the Voronoi cells model and microstructure fractals contacts surfaces new frontier applications. Science of Sintering, 2013, 45, 223-232.	1.4	10
140	Physico-chemical soil analysis of Rudovci region. Geonauka, 2013, 01, 1-8.	0.1	4
141	Intergranular area microalloyed aluminium-silicate ceramics fractal analysis. Science of Sintering, 2013, 45, 117-126.	1.4	4
142	Influence of prolonged sintering time on density and electrical properties of isothermally sintered cordierite-based ceramics. Science of Sintering, 2013, 45, 157-164.	1.4	8
143	Structural and electrical properties of Ti doped α-Fe2O3. Science of Sintering, 2013, 45, 281-292.	1.4	14
144	Investigation of sintering kinetics of magnesium titanate. Science of Sintering, 2013, 45, 133-139.	1.4	0

#	Article	IF	CITATIONS
145	ZnTiO3 ceramic nanopowder microstructure changes during compaction. Science of Sintering, 2013, 45, 209-221.	1.4	2
146	Study of dielectric behavior and electrical properties of hematite α-Fe2O3 doped with Zn. Science of Sintering, 2012, 44, 307-321.	1.4	30
147	Processing parameter influence on BaTiO <sub>3</sub> ceramic fractal microstructure and dielectric characteristics. Advances in Applied Ceramics, 2012, 111, 360-366.	1.1	7
148	Dehydration investigations of a refractory concrete using DTA method. Journal of Thermal Analysis and Calorimetry, 2012, 110, 37-41.	3.6	7
149	Comparison of structural properties of pristine and gamma irradiated single-wall carbon nanotubes: Effects of medium and irradiation dose. Materials Characterization, 2012, 72, 37-45.	4.4	30
150	Preparation of highly conductive carbon cryogel based on pristine graphene. Synthetic Metals, 2012, 162, 743-747.	3.9	26
151	Microstructural properties of electrochemically prepared Ni–Fe–W powders. Materials Chemistry and Physics, 2012, 135, 212-219.	4.0	14
152	Vertical distribution of natural radionuclides in soil: Assessment of external exposure of population in cultivated and undisturbed areas. Science of the Total Environment, 2012, 429, 309-316.	8.0	19
153	Influence of mechanochemical activation on the sintering of cordierite ceramics in the presence of Bi2O3 as a functional additive. Powder Technology, 2012, 218, 157-161.	4.2	35
154	Scanning electron microscopic examination of enamel surface after fixed orthodontic treatment: In-vivo study. Srpski Arhiv Za Celokupno Lekarstvo, 2012, 140, 22-28.	0.2	12
155	Mechanical-chemical synthesis Ba0.77Sr0.23TiO3. Science of Sintering, 2012, 44, 47-55.	1.4	5
156	Synthesis of barium-zinc-titanate ceramics. Science of Sintering, 2012, 44, 65-71.	1.4	3
157	The influence of mechanical activation on sintering process of BaCO3-SrCO3-TiO2 system. Science of Sintering, 2012, 44, 271-280.	1.4	5
158	Isothermal sintering of barium–zinc–titanate ceramics. Ceramics International, 2011, 37, 21-27.	4.8	5
159	Structural investigation of mechanically activated nanocrystalline BaTiO3 powders. Ceramics International, 2011, 37, 2513-2518.	4.8	15
160	Analysis and modeling of sintering of Sr-hexaferrite produced by PIM technology. Science of Sintering, 2011, 43, 9-20.	1.4	4
161	Isothermal kinetics of titanium-oxo-alkoxy clusters formation. Science of Sintering, 2011, 43, 95-104.	1.4	1
162	Sintering of mechanically activated magnesium-titanate and barium-zinc-titanate ceramics. Science of Sintering, 2011, 43, 145-151.	1.4	6

#	Article	IF	CITATIONS
163	Electrical properties and microstructure fractal analysis of magnesium-modified aluminium-silicate ceramics. Science of Sintering, 2011, 43, 193-204.	1.4	5
164	Sintering process influence on microstructure and intergranular impedance of rare-earth modified BaTiO3-ceramics. Science of Sintering, 2011, 43, 277-287.	1.4	6
165	ROS-inducing potential, influence of different porogens and in vitro degradation of poly (D,L-lactide-co-glycolide)-based material. EXPRESS Polymer Letters, 2011, 5, 996-1008.	2.1	17
166	Impedance Response and Dielectric Relaxation in Liquid-Phase Sintered Zn2SnO4-SnO2 Ceramics. Journal of Electronic Materials, 2010, 39, 447-455.	2.2	17
167	Influence of Rareâ€Earth Dopants on Barium Titanate Ceramics Microstructure and Corresponding Electrical Properties. Journal of the American Ceramic Society, 2010, 93, 132-137.	3.8	87
168	Microstructure evolution and phase transition in La/Mn doped barium titanate ceramics. Processing and Application of Ceramics, 2010, 4, 253-258.	0.8	8
169	Structure and composition of soils. Processing and Application of Ceramics, 2010, 4, 259-263.	0.8	10
170	Influence of mechanical activation on microstructure and crystal structure of sintered MgO-TiO2 system. Science of Sintering, 2010, 42, 143-151.	1.4	19
171	Application of the intergranular impedance model in correlating microstructure and electrical properties of doped BaTiO3. Science of Sintering, 2009, 41, 247-256.	1.4	15
172	Nickel-based super-alloy Inconel 600 morphological modifications by high repetition rate femtosecond Ti:sapphire laser. Laser and Particle Beams, 2009, 27, 699-707.	1.0	9
173	Light transmission through fiber post: The effect on adhesion, elastic modulus and hardness of dual-cure resin cement. Dental Materials, 2009, 25, 837-844.	3.5	56
174	Structural and electrical properties of sintered zinc-titanate ceramics. Ceramics International, 2009, 35, 35-37.	4.8	16
175	Influence of mechanical activation on the structure of ultrafine BaTiO3 powders. Journal of Alloys and Compounds, 2009, 486, 633-639.	5.5	21
176	Influence of mechanical activation on structural and electrical properties of sintered MgTiO3 ceramics. Science of Sintering, 2009, 41, 117-123.	1.4	4
177	Morphology investigation of mechanically activated ZnO–SnO2 system. Ceramics International, 2008, 34, 639-643.	4.8	15
178	Microstructural evolution and electric properties of mechanically activated BaTiO3 ceramics. Journal of the European Ceramic Society, 2007, 27, 575-579.	5.7	20
179	Photoacoustic spectroscopy investigation of sintered zinc-tin-oxide ceramics. Hemijska Industrija, 2007, 61, 142-146.	0.7	1
180	The Influence of Tribophysical Activation on Non-Isothermal Sintering of BaTiO <sub>3</sub> Ceramics. Materials Science Forum, 2006, 514-516, 1566-1570.	0.3	1

#	Article	IF	CITATIONS
181	Contribution of Frenkel's theory to the development of materials science. Science of Sintering, 2006, 38, 3-6.	1.4	2
182	Analysis of early-stage sintering mechanisms of mechanically activated BaTiO3. Science of Sintering, 2006, 38, 239-244.	1.4	4
183	Application of the Master Sintering Curve Theory to Non-Isothermal Sintering of BaTiO <sub>3</sub> Ceramics. Materials Science Forum, 2005, 494, 417-422.	0.3	15
184	Correlation Between Densification Rate and Microstructure Evolution of Mechanically Activated BaTiO3. Ferroelectrics, 2005, 319, 75-85.	0.6	24
185	DPR Analysis of Microstructural Evolution of ZnO Ceramics. Materials Science Forum, 2004, 453-454, 453-458.	0.3	1
186	Electrical properties of screen printed BaTiO3 thick films. Journal of the European Ceramic Society, 2004, 24, 1467-1471.	5.7	22
187	Phase Transformations and Thermal Effects of Mechanically Activated BaCO 3 -TiO 2 System. Ferroelectrics, 2002, 271, 391-396.	0.6	5
188	Barium titanate screen-printed thick films. Ceramics International, 2002, 28, 293-298.	4.8	54
189	Low temperature sintering of mechanically activated BaCO3-TiO2. Science of Sintering, 2002, 34, 73-77.	1.4	7
190	Screen Printed Barium Titanate Thick Films Prepared from Mechanically Activated Powders. Key Engineering Materials, 2001, 206-213, 1425-1428.	0.4	1
191	Grain growth during sintering of BaTiO3 with LiF. Ferroelectrics, 1996, 186, 165-168.	0.6	6
192	Distribution of natural radionuclides in anthrosol-type soil. Turk Tarim Ve Ormancilik Dergisi/Turkish Journal of Agriculture and Forestry, 0, , .	2.1	7